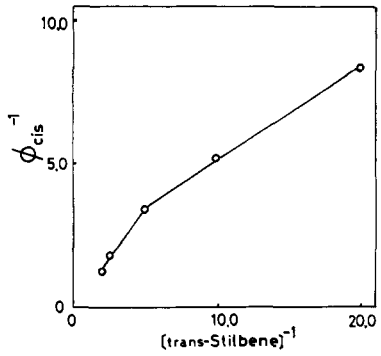


**Figure 6.** Stern-Volmer relationship in the trans → cis isomerization of stilbene catalyzed by the $[Cu(CH_3CN)_4]^+$-phen system; $[[Cu(CH_3CN)_4]^+] = 5 \times 10^{-3}$ mol/dm$^3$, [phen] = $2.5 \times 10^{-3}$ mol/dm$^3$, and the L-39 and C-40C cutoff filters were used.

eq 3 is small. However, this mechanism needs the energy transfer between transition-metal complexes, which is usually considered to be novel. Scheme I does not require such energy transfer and seems more probable. However, this mechanism cannot explain the maximum activity at [biL]/$[Cu(CH_3CN)_4]^+$ = 0.5, when eq 3 operates little at [biL]/$[Cu(CH_3CN)_4]^+$ = 0.5-1.0.

Finally, the Stern-Volmer relationship was examined, by using the $[Cu(CH_3CN)_4]^+$-phen system. As is shown in Figure 6, the good linear relationship is found at low concentrations of *trans*-stilbene, but the downward deviation occurs at high concentrations of *trans*-stilbene. This feature of the Stern-Volmer relation generally suggests that the variance of the operating mechanism and/or the active species depends on the concentration of *trans*-stilbene. At low concentrations of *trans*-stilbene, equilibria 2-4 are operating, in which the concentration of $[Cu(CH_3CN)_3(trans\text{-stil})]^+$ and $[Cu(biL)(CH_3CN)(trans\text{-stil})]^+$ increases with increasing concentration of *trans*-stilbene, leading to an increase of $\phi_{cis}$ values in either the mechanism of Scheme I or that of Scheme II. Thus, an increase in $\phi_{cis}$ with increasing *trans*-stilbene concentration, shown in Figure 6, is qualitatively explained. At sufficiently high concentrations of *trans*-stilbene, equilibria 7-10 become operating. Resulting species, $[Cu(biL)(trans\text{-stil})_2]^+$ and $[Cu(CH_3CN)_m(trans\text{-stil})_{4-m}]^+$ ($m < 3$) are considered to be more effective for the *trans*-stilbene isomerization than $[Cu(biL)(CH_3CN)(trans\text{-stil})]^+$ and $[Cu(CH_3CN)_3(trans\text{-stil})]^+$, for the increasing numbers of coordinating *trans*-stilbenes increase the probability that *trans*-stilbene participates in the excitation resulting from energy transfer, intersystem crossing, or internal conversion. Consequently, the $\phi_{cis}^{-1}$ value deviates downward at sufficiently high concentrations of *trans*-stilbene. A further discussion is omitted here, because the present system has complicated equilibria and the relation between $\phi_{cis}^{-1}$ and [*trans*-stilbene]$^{-1}$ cannot be derived here.

**Concluding Remarks.** New Cu(I) photocatalysts, prepared in situ from $[Cu(CH_3CN)_4]^+$ and biL (biL = 2,2′-bipyridine, 1,10-phenanthroline, and their derivatives), are presented in this work. These catalysts are the first examples of Cu(I) photocatalysts efficient upon irradiating with visible light (>390 nm) and are as good as $[Ru(bpy)_3]^{2+}$ if the quantum yield for *cis*-stilbene formation and the *cis*-stilbene/*trans*-stilbene mole ratio at a photostationary state are considered. Thus, further application to the other reaction is expected to be possible. Two kinds of reaction mechanisms are presented: In one, the active species is $[Cu(biL)(CH_3CN)(trans\text{-stil})]^+$ and the trans → cis isomerization of stilbene proceeds in the excited state of this complex resulting from the visible light absorption. In the other, the Cu(I)-biL complexes absorb the visible-light energy and transfer it to $[Cu(CH_3CN)_3(trans\text{-stil})]^+$, in whose excited state the trans → cis isomerization proceeds. Experimental results are explainable for both mechanisms, but the former mechanism seems more probable, for this mechanism does not need the novel energy transfer between transition-metal complexes.

**Acknowledgment.** We wish to thank the reviewers for instructive suggestions about the reaction mechanism.

**Registry No.** $[Cu(CH_3CN)_4]ClO_4$, 14057-91-1; bpy, 366-18-7; phen, 66-71-7; 2,9-dmp, 484-11-7; 4,7-dmp, 3248-05-3; 4,7-dpp, 1662-01-7; *cis*-stilbene, 645-49-8; *trans*-stilbene, 103-30-0.

Contribution from Frick Laboratory,
Department of Chemistry, Princeton University, Princeton, New Jersey 08544

# Reaction of Nickel Electrode Surfaces with Anionic Metal-Cyanide Complexes: Formation of Precipitated Surfaces

SUJIT SINHA, BRIAN D. HUMPHREY, and ANDREW B. BOCARSLY*

*Received July 7, 1983*

Anionic metallocyanide complexes ($Fe(CN)_6^{3-}$, $Ru(CN)_6^{3-}$, $Mn(CN)_6^{3-}$, $[Fe(CN)_{6-x}L_x]^{n-}$) (L = $H_2O$, NO, histidine, 1,2-cyclohexyldiamine) capable of precipitating aqueous $Ni^{2+}$ are immobilized on Ni electrodes by potentiostating the electrode in aqueous solutions of the anions. The surface coverage obtained is shown to be a function of composition of derivatizing solution, nickel surface pretreatment, electrode potential, and the reaction time. Diffuse-reflectance FT IR spectra of derivatized Ni surfaces show a cyano-bridged bimetallic structure. The cyclic voltammograms of surface-immobilized $Fe(CN)_6^{3-}$ and $Ru(CN)_6^{3-}$ show zero peak to peak separation and 110-mV peak width at half-height, close to the ideal case for surface-attached species. These surfaces are very stable with ~10% loss on >18 000 potential cycles between the $Fe^{II}$ and $Fe^{III}$ states. The $E_{1/2}$ value and the shape of the surface cyclic voltammetric wave are shown to depend strongly on the supporting electrolyte cation. These surfaces also show a cation selectivity, indicating an ordered structure. Such surfaces are shown to stabilize the Ni electrode surface against oxide formation while allowing various solution redox couples to react at the electrode. Thus, reaction specificity can be induced by this type of derivatization.

It is now well established that surface derivatization techniques can be employed to synthesize electrochemical interfaces having specific charge-transfer properties. Such techniques have been applied to both standard electroanalytical electrode materials[1] and various photosensitive semiconducting electrodes.[2] Very little effort, however, has been exerted to apply these approaches to the modification and control of

(1) Murray, R. W. *Acc. Chem. Res.* **1980**, *13*, 135.
(2) Wrighton, M. S. *Acc. Chem. Res.* **1979**, *12*, 303.

0020-1669/84/1323-0203$01.50/0 

interfacial charge transfer at reactive metal surfaces. The success obtained using other electrode surfaces though suggests that application of surface-modification techniques to highly nonnoble charge-transfer interfaces may provide an approach for converting relatively poor, yet inexpensive, electrode materials into good electrodes. Further, such procedures may allow one to take advantage of the surface properties of these materials to carry out new electrochemical processes. In order to exploit this situation one must be able to synthesize not only an interface with a high degree of stability but one that can suppress nondesirable surface reactions such as corrosion, without inhibiting desirable interfacial charge-transfer processes.

Recently we reported a preliminary account dealing with the modification of established anodic film formation techniques to yield novel redox-active surface species on oxidatively unstable electrodes.[3] A nickel interface was employed as the model system. Our approach was based on utilizing the metal ions formed during the corrosion process as one of the derivatization reagents. These surface-bound metal ions were used to "precipitate" an appropriate surface species onto the electrode. Empirically we found that several species of the form $[M(CN)_5L]^{n-}$ (M = Fe, Ru) could be immobilized on a Ni electrode under either anodizing electrochemical or chemical conditions. The surfaces so formed showed a high degree of stability. Since that report we have observed that appropriately derivatized surfaces can carry out a number of interfacial redox reactions found impossible at the native surface. Further, we have found the formation of such surfaces at the Ni interface is rather general with respect to the complex anion employed, and thus the interfacial character can easily be modified in a variety of different ways. This includes changing not only the central metal involved but the ligand coordination sphere itself. Thus, the approach to surface derivatization offered herein is not limited to the placement of a specific complex type on the nickel surface but can be considered a general method for derivatizing oxidatively unstable surfaces. As an example of the general scope of this approach we consider the placement of an L-histidine group on the electrode surface via reaction of a nickel electrode with $[Fe(CN)_5His]^{3-}$ (L-histidine ≡ His).

These surfaces are superficially similar to Prussian Blue derivatized surfaces recently reported by Neff,[4] Itaya,[5] Rosseinsky,[6] and Kuwana.[30] The nickel ferricyanide complexes formed on the surfaces under discussion can be considered a mixed-metal analogue of Prussian Blue. However, there exists a significant difference between these two types of surfaces. That is, the surfaces presented here are formed as an intrinsic part of the metal interface, they are not a simple coating as are the Prussian Blue surfaces. This factor leads to two major differences. The first is that a much higher degree of synthetic control can be exerted during the derivatization of the nickel surface with respect to both amount and structure of surface material. The second is that the electrochemistry observed is quite different. For example, recently we reported an unique and unprecedented cation selectivity for $Ni/Fe(CN)_6^{4-/3-}$ and $Ni/Ru(CN)_6^{4-/3-}$ surfaces that cannot be explained using simple equilibrium arguments.[7] Similarly the details of the electroanalytical behavior of the two types of surfaces are different; the Ni-based surfaces show a much higher degree of ideality than most previously reported derivatized electrodes as will be discussed. Finally, it should be noted that the methodology described leads to the synthesis of surfaces that allow a classically unstable electrode material to behave in many ways like an analytical electrode material. Similar results cannot be obtained by simple coating techniques such as the deposition of Prussian Blue overlayers.

Herein we report the details and scope of the surface synthesis along with a characterization of both the charge transfer and chemical properties of the surfaces formed. Further, we discuss the mechanism of surface formation and the relationship between surface structure and interfacial charge transfer. Since the chemical modification under consideration can be affected by using electrochemical techniques, the surfaces formed are subject to a high degree of reproducibility. Synthetic flexibility combined with reproducibility has allowed assessment of surface properties often elusive in other surface-modification studies.

## Preparation and Synthetic Scope

**(a) Derivatizing Reagents.** Empirically we find that any species that rapidly precipitates in the presence of aqueous $Ni^{2+}$ can be placed on a nickel electrode surface. Thus, complexes such as $[Fe(CN)_5L]^{n-}$ (L = CN, $H_2O$, NO, histidine), $[Mn(CN)_6]^{3-}$, and $[Ru(CN)_6]^{3-}$ have been successfully bound to Ni electrodes. However, complexes such as $[Mo(CN)_8]^{3-}$, which only slowly form a precipitate with $Ni^{2+}$, or $[Fe(bpy)_2(CN)_2]^{+}$, which forms a soluble complex with $Ni^{2+}$, have not been successfully surface attached. Besides this criteria it is also found that electrodes can be derivatized by simple dipping in aqueous solution of the metal complex if the complex is in an oxidation state capable of oxidizing $Ni^0$. For example, derivatization by dipping occurs with $[Fe(CN)_6]^{3-}$ but not $[Fe(CN)_6]^{4-}$. Further, it is found that while species such as $[Ru(CN)_6]^{4-}$ cannot be surface attached by this procedure, the material can be placed on a nickel surface by dipping in a solution containing both $[Fe(CN)_6]^{3-}$ and $[Ru(CN)_6]^{4-}$. (Both species are observed on the surface.) This supports the idea that surface oxidation is a necessary step in the derivatization procedure and provides a first line of evidence that species of the form $[Ni^{II}_x(M(CN)_5L)_y]^{n-}$ are the actual surface species.

**(b) Derivatization Procedure.** The amount of material that can be loaded onto a surface and the electrochemical properties of the surface were found to be highly dependent upon the initial preparation of the electrode surface. Electrodes that were untreated did yield surface species upon dipping in a solution of the derivatizing agent and an oxidant as described above; however, low, unpredictable coverages were obtained. This situation could be improved to some extent by abrading the electrodes just prior to dipping, suggesting that natural oxides on the surface inhibited the derivatization procedure. That this was the case was verified by electrochemically synthesizing various surface oxides in 1 M NaOH electrolyte[8,9] and testing the ability of oxide-coated electrodes to pick up $K_3Fe(CN)_6$. All oxide coatings lead to a massive decrease in the surface coverage obtainable.

(3) Bocarsly, A. B.; Sinha, S. *J. Electroanal. Chem. Interfacial Electrochem.* **1982**, *137*, 157.
(4) (a) Neff, V. D. *J. Electrochem. Soc.* **1978**, *125*, 887. (b) Ellis, D.; Eckhoff, M.; Neff, V. D. *J. Phys. Chem.* **1981**, *85*, 1225. (c) Rajan, K. P.; Neff, V. D. *J. Phys. Chem.* **1982**, *86*, 4361.
(5) (a) Itaya, K.; Shibayam, K.; Akahoshi, H.; Toshima, S. *J. Appl. Phys.* **1982**, *53*, 804. (b) Itaya, K.; Akahoshi, H.; Toshima, S. *J. Electrochem. Soc.* **1982**, *129*, 1498. (c) Itaya, K.; Ataka, T.; Toshima, S. *J. Am. Chem. Soc.* **1982**, *104*, 3751; **1983**, *104*, 4768. (d) Itaya, K.; Ataka, T.; Toshima, S. *J. Phys. Chem.* **1982**, *86*, 2415.
(6) Kellawi, H.; Rosseinsky, D. R. *J. Electroanal. Chem. Interfacial Electrochem.* **1982**, *131*, 373.
(7) Bocarsly, A. B.; Sinha, S. *J. Electroanal. Chem. Interfacial Electrochem.* **1982**, *140*, 167.
(8) Bocarsly, A. B.; Galvin, S. A. Sinha, S. "The Nickel Electrode"; Gunther, R. G., Gross, S., Eds.; The Electrochemical Society: New York, 1983; Vol. 82–4, pp 97–117.
(9) (a) Weininger, J. L.; Breiter, M. W. *J. Electrochem. Soc.* **1963**, *110*, 484; **1964**, *111*, 707. MacArthur, D. M. *Ibid.* **1970**, *117*, 422. (c) Hopper, M. A.; Ord, J. L. *Ibid.* **1973**, *120*, 183. (d) Guzman, R. S. S.; Vilche, J. R.; Arvia, A. J. *Ibid.* **1978**, *125*, 1578. (e) Wolf, J. F.; Yeh, L. S. R.; Damjanovic, A. *Electrochim. Acta* **1981**, *26*, 409; **1981**, *26*, 811.

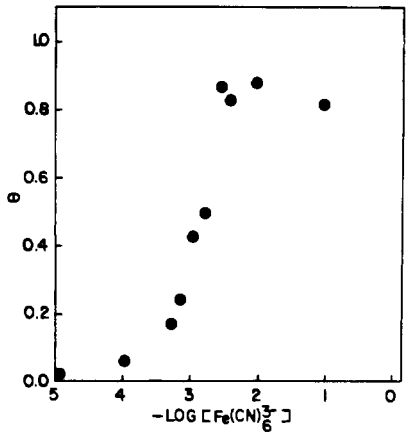


**Figure 1.** Dependence of coverage on solution concentration of $Fe(CN)_6^{3-}$. The fractional coverage, $\theta$, is defined at $\Gamma/\Gamma_{max}$ where $\Gamma_{max} = 3.5 \times 10^{-8}$ mol/cm$^2$. Data points were taken after a 60-s derivatization period. Each point represents the average of three electrode values.

Although the removal of oxide by abrasion does enhance surface coverage, it does not cure the reproducibility problem. Further, the dipping procedure leads to a very complicated electrochemical interface. In order to overcome these problems and develop a more general procedure for attaching species onto the Ni interface, a second approach was adopted. The method involved potentiostating the Ni electrode anodically in the presence of the derivatizing reagent in aqueous electrolyte. This technique yielded extremely reproducible surfaces as long as the reaction parameters (surface pretreatment, electrode potential, reaction time, electrolyte composition) were held constant. Further, this technique produced surface-attached species for all precipitable $[M(CN)_{6-x}L_x]$ complexes.

Anodization of an electrode in a cell containing only supporting electrolyte leads to oxide formation via interaction of the surface $Ni^{2+}$ with oxygen-containing species.[10] This process is suppressed to some degree upon addition of the derivatizing reagent, indicating that derivatization process is competitive with oxide formation under the neutral to slightly acidic conditions employed (pH 3–7). However, it is reasonable to assume that some surface oxide is generated during the derivatization procedure and that oxide formation during anodization plays a role in the final surface morphology. This effect has been minimized by employing a pH range where nickel oxides are fairly unstable.[11]

Besides electrolyte pH the exact concentration of derivatizing reagent is important in determining the final surface loading obtained. As can be seen in Figure 1 for $[Fe(CN)_6]^{3-}$, fractional surface coverage, $\theta$ (as determined by cyclic voltammetry),[12] vs. solution concentration follows a sigmoidal curve, with the plateau region ($\theta = 1$) corresponding to a maximum coverage of ~250 monolayers. Note that the plot indicates a saturation effect at solution concentrations greater than $\sim 5 \times 10^{-3}$ M. Optimum results were obtained by using concentrations in the range of $\sim 1 \times 10^{-3}$ M. No pickup could be detected at concentrations less than $10^{-5}$ M. Similarly we have found that, at low to moderate concentrations, stirring the electrolyte inhibits surface formation. These results are consistent with the idea that the surface-formation reaction is a precipitation type reaction requiring specific minimum concentrations of $[Fe(CN)_6]^{3-}$ and surface $Ni^{2+}$; stirring may serve to remove a significant portion of the electrochemically generated $Ni^{2+}$ from the surface or near-surface region into the bulk electrolyte. Stable interfaces can only be formed when nickel ions are present in sufficient quantities at the electrode surface. Although addition of $Ni^{2+}$ to a solution containing $[Fe(CN)_6]^{3-}$ and a nickel electrode causes a visible precipitate to form on the electrode, no stable electrochemistry is observed. Similarly, the final surface coverage can also be regulated by controlling the reaction time. As is shown in Figure 2, there is an exponential dependence of surface coverage on reaction time as is expected for a first-order reaction. This first-order dependence is maintained as long as the concentration of solution complex is kept above $4 \times 10^{-4}$ M indicative of pseudo-first-order kinetics.

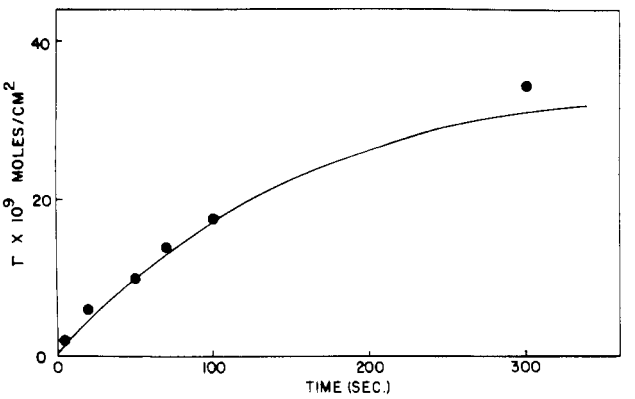


**Figure 2.** Coverage vs. time data (solid circles) for the potentiostatic formation of $Ni/Fe(CN)_6^{3-}$, in 2.5 mM $[Fe(CN)_6]^{3-}$. The electrode potential is 1.8 V vs. SCE, and the reaction is maintained at room temperature. Each data point represents the average of four experiments. Coverage is determined by cyclic voltammetry.

**Table I.** Effect of Cation Concentration on Surface Coverage

| $[K_3Fe(CN)_6]$, M | [added $K^+$],[a] M | $10^9\Gamma$,[b] mol/cm$^2$ |
|---|---|---|
| $10^{-3}$ | 0 | 7.0 |
| | 0.1 | 9.0 |
| | 1 | 6.6 |
| $10^{-4}$ | 0 | 3.2 |
| | 0.1 | 0.6 |
| | 1 | ~0 |
| $10^{-5}$ | 0 | 0.35 |
| | 0.1 | ~0 |

[a] Note there is a 3:1 molar ratio of $K^+$ to $[Fe(CN)_6]^{3-}$ in the absence of added $K^+$. [b] Determined by cyclic voltammetry.

Beside the expected dependence on the concentration of derivatizing reagent present, a dependence on the concentration of supporting electrolyte is observed. This is demonstrated in Table I for $K_3Fe(CN)_6$ derivatizing reagent containing $KNO_3$ supporting electrolyte. At high concentrations of $K_3Fe(CN)_6$ the effect is small while at concentrations <0.001 M a strong dependence is observed. At extremely low concentrations of $K_3Fe(CN)_6$, electrode pickup can be totally suppressed by addition of $KNO_3$. Once formed, however, the surfaces are not subject to degradation by exposure to various salts. Addition of ions to the derivatizing electrolyte apparently induces a competition reaction for available surface sites. The exact nature of the competition is unclear; however, it is associated with the cations present since variation in the anions employed has no effect while different cations show slightly different responses. This salt effect is not associated with contact-pair formation between the cation and the complex anion since, for the case of $K^+$ vs. $Ba^{2+}$ with $[Fe(CN)_6]^{3-}$, the $K^+$ appears to have a larger effect than the $Ba^{2+}$, yet the

(10) MacGougall, B.; Graham, M. J. *J. Electrochem. Soc.* **1981**, *128*, 2321.
(11) Arvia A. J.; Posadas, D. "Encyclopedia of Electrochemistry of the Elements"; Bard, A. J., Ed.; Marcel Dekker: New York, 1975; Vol. 3, p 212.
(12) Surface coverage has been determined by integration with respect to time of the area under the anodic cyclic voltammetric curve. The values so obtained were found to be independent of scan rate and verifiable by chronocoulometry. An appropriate base line correction was made.[1] Monolayer coverage was assigned on the basis of the single-crystal X-ray structure for $K_2[Ni(NC)Fe(CN)_5]$.[32]

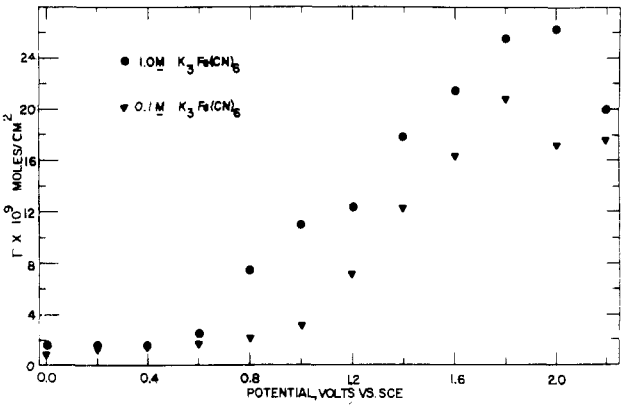


**Figure 3.** Surface coverage as a function of electrode potential and derivatizing reagent concentration. Derivatization was carried out for a 60-s period.

$Ba^{2+}$–$Fe(CN)_6^{3-}$ ion pair is favored by ~30-fold under equilibrium conditions.[13]

As might be expected the final coverage obtained is also a strong function of the potential employed. The correlation between surface coverage and potential is illustrated for $[Fe(CN)_6]^{3-}$ in Figure 3. At potentials greater than +1.8 V vs. SCE the surface coverage changes very little. The coverage at potentials greater than +1.4 V vs. SCE shows some scatter since surface formation competes with $O_2$ evolution in this region. In the region from +0.6 V vs. SCE to +1.8 V vs. SCE, the coverage obtained is a fairly linear function of potential. This allows for straightforward control of electrode coverage, thus enhancing the synthetic aspects of this procedure. Presumably this linear dependence reflects the surface density of the $Ni^{2+}$ species. At potentials above +1.8 V vs. SCE the rate of $Ni^{2+}$ formation is apparently saturated while below +0.6 V vs. SCE the surface coverage is minimal, suggesting that this is the onset potential for $Ni^{2+}$ formation. The small coverage obtained at potentials negative of this potential reflects pickup associated with the "dipping" experiment. If one employs a reduced species in the electrolyte, no pickup in this region is observed. The coverage vs. potential plot is to some extent dependent on the derivatizing agent employed. This is to be expected since surface species formation should be associated with the formation equilibrium constant for the binuclear bridged species and thus vary with the complex employed and the concentration of $Ni^{2+}$. For the specific case of $[Fe(CN)_6]^{3-}$, this dependence can be seen by comparing the coverage vs. potential plot for two different concentrations of complex (Figure 3). Note the two curves are essentially parallel to each other but shifted in potential ($Ni^{2+}$ concentration), thus compensating for variations in $[Fe(CN)_6]^{3-}$ concentration. Beside effects associated with $Ni^{2+}$ concentration, the potential may also control surface formation by double-layer effects that might regulate either concentrations of reactants in the near-surface region or the surface structure formed during the reaction.

Finally, it should be noted that the procedures employed are not restricted to putting a single species on the electrode surface. Multiple-surface species can be obtained either by potentiostating the electrode in an electrolyte containing all of the species of interest or by carrying out a series of anodizations each in a one-component electrolyte.

### Surface Characterization

**(a) Spectroscopic Properties.** Direct evidence as to the nature of the surface species and mechanism of surface formation can be obtained spectroscopically. Two experiments were carried out to characterize the surface. The first spectroscopic procedure employed, as has been previously reported,[3] involved derivatization of high-surface-area nickel powder by using the "dipping" technique, followed by washing with water until the wash water was free of derivatizing reagent. The surface was then treated with 1 M NaOH solution to remove all surface-attached material. The composition of the base wash was monitored via UV–visible spectroscopy. Although indirect, this technique allowed for a measurement of the amount of surface-attached material. Further, with use of this approach electrochemically inactive complexes could be tested for their derivatizing ability. A comparison of the results obtained by using this technique with the electrochemical results indicates that for those systems that were electroactive, within experimental error, all of the surface-confined material is electroactive. This appears rather unusual when compared with other derivatized surfaces such as those made by silylation techniques or spin coating of polymers, in which it has often been noted that a fair amount of the surface material is electrochemically silent. Perhaps, more interestingly we find that although the surface reagent must be in a high oxidation state in order to be surface attached, it is always in the reduced state after removal. This provides compelling evidence for the redox mechanism of surface formation put forth earlier. Although the data do not directly demonstrate that $Ni^0$ is the reducing agent, it is the only material present that is thermodynamically capable of reducing the complexes employed ($E_R$ = −0.47 V vs. SCE).[11]

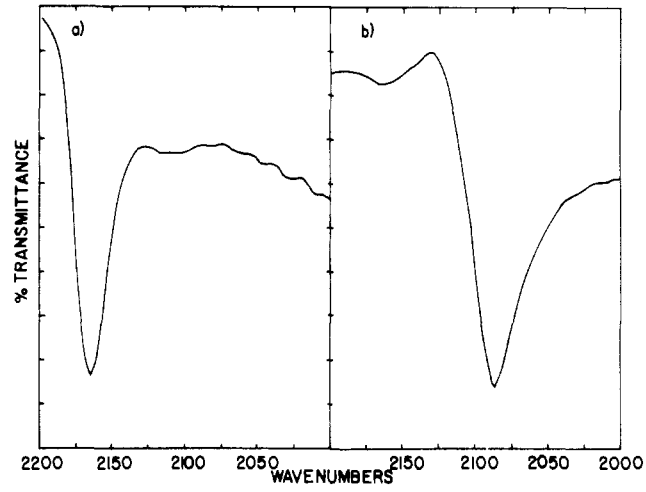


**Figure 4.** (a) Diffuse-reflectance FT IR spectrum of the nickel electrode derivatized with $[Fe(CN)_6]^{3-}$ and potentiostated anodic of the surface $E_{1/2}$ prior to recording of the spectrum. (b) Spectrum of the electrode in part a potentiostated cathodic of the surface $E_{1/2}$ prior to recording of the spectrum. Spectra were observed from 4000 to 500 cm$^{-1}$. The only portion showing reproducible peaks is illustrated above. Spectra are referenced against a clean nickel electrode. There were 128 scans collected per spectrum.

The second spectroscopic approach, diffuse reflectance FT IR, was used to directly detect the species present on the electrode as a function of its electrochemical history. Spectroscopic experiments were carried out in air, not in the electrochemical cell, and therefore there is some question as to whether or not the observed spectra correspond to the actual electrochemical surface species. We have carried out a large number of experiments however, electrochemically monitoring the electrodes before and after the spectroscopic experiment to ensure that our procedure does not perturb the surface. A typical spectroscopic result for nickel derivatized with $[Fe(CN)_6]^{3-}$ is shown in Figure 4a. A single transition is observed at 2164 cm$^{-1}$. This absorption is only obtained if the electrode has been derivatized. Washing the derivatized electrode with 1 M NaOH causes the IR signal to disappear, confirming that

(13) Bjerrum, J.; Schwarzenbach, G.; Sillen, L. G. "Stability Constants"; Chemical Society: London, 1958.

Table II. Diffuse-Reflection FT IR Results for Surface-Bound Species and Model Compounds

| compd | metal oxidn state | IR bands (CN str), $cm^{-1}$ |
|---|---|---|
| $K_3Fe(CN)_6$ | Fe(III) | 2122, 2091, 2075 |
| $KNiFe(CN)_6$ | Fe(III) | 2174 |
| $K_4Fe(CN)_6$ | Fe(II) | 2091, 2068, 2029 |
| $K_2NiFe(CN)_6$ | Fe(II) | 2114 |
| $Na_2Fe(CN)_5H_2O$ | Fe(III) | 2075, 2041 |
| $NiFe(CN)_5H_2O$ | Fe(III) | 2172, 2110 |
| $Na_2Fe(CN)_5NO$ | Fe(III) | 2172, 2160, 2145, 1967,[d] 1933,[d] 1909[d] |
| $NiFe(CN)_5NO$ | Fe(III) | 2207, 1960, 1925 |
| $NiFe(CN)_5His$ | Fe(III) | 2187, 2110 |
| $K_4Ru(CN)_6$[a] | Ru(II) | 2085, 2073, 2043 |
| II. Surface Species | | |
| $[Fe(CN)_6]^{3-}$ | Fe(III) | 2164 |
| $[Fe(CN)_6]^{4-}$ | Fe(II) | 2091,[c] 2087, 2083 |
| $[Fe(CN)_5H_2O]^{3-}$ | Fe(II) | 2091 |
| $[Fe(CN)_5NO]^{2-}$[b] | Fe(III) | 2191, 1925[d] |
| $[Fe(CN)_5His]^{2-}$ | Fe(III) | 2164 |
| $[Fe(CN)_5His]^{3-}$ | Fe(II) | 2083 |
| $[Ru(CN)_6]^{4-}$ | Ru(II) | 2098,[c] 2095 |

[a] Both the redox and ligand substitution instability of the Ru(III) species made it impossible to observe this species under the conditions employed. [b] This species is not electroactive, and thus, only the Fe(III) state was studied. [c] Only one band is observable; however, it shifts slightly with electrode preparation (time, potential, etc.). For a given preparative method, the peak frequency is reproducible. [d] NO stretching frequencies.

the transition is associated with the derivative. The absorption band falls in the region expected for a bridging cyanide ligand, not a terminal species,[14a] offering direct evidence that the bridged dinuclear [Ni, Fe] species is present on the surface. Further, we find an absorption identical with those of authentic samples of $KNi^{II}Fe^{III}(CN)_6$. The data are also in agreement with literature spectra of $[Ni^{II}Fe^{III}(CN)_6]^-$[14b] and the IR spectrum obtained by Neff of Prussian Blue[4b] (a cyanide-bridged [$Fe^{II}$, $Fe^{III}$] dimer) on a gold substrate. If the electrode is reduced, forming a $[Fe(CN)_6]^{4-}$ surface species, the spectrum converts to that shown in Figure 4b, the transition shifting to 2087 $cm^{-1}$. This is the expected result since reduction to an $Fe^{II}$ species yields a filled $Fe^{II}$ $t_{2g}$ MO, thereby enhancing metal back-bonding into the cyanide $\pi^*$ orbital and thus reducing the carbon–nitrogen bond strength. This observation is supported by IR data on an authentic sample of $K_2Ni^{II}Fe^{II}(CN)_6$ and the literature cited above. Similar results are obtained for $[Ru(CN)_6]^{4-/3-}$ as shown in Table II. Quite surprisingly for both $[Ru(CN)_6]^{4-/3-}$ and $[Fe(CN)_6]^{4-/3-}$ no indication of the presence of terminal $CN^-$ is detected. This may be interpreted as evidence either that most of the $CN^-$ ligands are bridged or that surface-associated selection rules are suppressing these vibrations. A comparison of the ligand stretching region of various derivatizing reagents, model nickel salts of those reagents, and the actual surface spectra (Table II) indicates that both the binding of a $Ni^{2+}$ ion to the anionic complex and the actual surface environment serve to lower the number of transitions observed. This phenomenon is not simply due to a lack of sensitivity in the experimental apparatus since bands showing similar oscillator strengths for the model nickel compounds exhibit very different intensities on the electrode surface. For example, the 1960- and 1925-$cm^{-1}$ bands in $Ni^{II}Fe^{III}(CN)_5NO$, which are associated with the NO stretch,[15] are of similar intensity; however, only the 1925-$cm^{-1}$ band is observed on the surface. Therefore, either geometric distortions of the surface complex are occuring or the nature of the interface requires changes in the selection rules.

On the other hand, it seems reasonable to expect that some indication of a terminal $CN^-$ group would be obtained if it existed in reasonable concentration. The loading of surface species (~100 monolayers) is sufficiently high that minimally the outer layers should be relatively unperturbed by the nickel surface. That terminal cyanides are not observed suggests the surface is composed of a relatively ordered nickel metallocyanide lattice (crystalline) on a nickel substrate. Such a surface might be expected to have certain properties that reflect its crystalline nature. As discussed below the surfaces exhibit a unique cation specificity, which appears associated with such a structure.

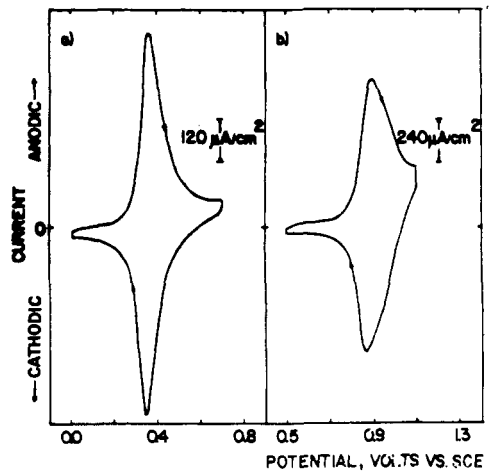


Figure 5. Cyclic voltammograms of chemically modified nickel surfaces in supporting electrolyte containing 0.1 M $NaNO_3$ and no deliberately added electroactive material (scan rates 100 mV/s): (a) $[Fe(CN)_6]^{4-/3-}$; (b) $[Ru(CN)_6]^{4-/3-}$.

Table III. Representative Cyclic Voltammetric Data[a]

| surface species[b] | $10^9\Gamma$, mol/cm² | $E_{1/2}$, mV (vs. SCE) | $\Delta E$,[c] mV | fwhh, mV anodic | fwhh, mV cathodic |
|---|---|---|---|---|---|
| $[Fe(CN)_6]^{4-/3-}$ | 3.0 | 355 | 15 | 180 | 115 |
| | 7.0 | 355 | 10 | 115 | 100 |
| | 12.0 | 355 | 35 | 110 | 110 |
| | 18.0 | 355 | 35 | 110 | 100 |
| | 24.0 | 355 | 45 | 120 | 115 |
| | 40.0 | 355 | 70 | 140 | 120 |
| $[Mn(CN)_6]^{3-/2-}$ | 2.0 | 1000 | 90 | *d* | 250 |
| $[Ru(CN)_6]^{4-/3-}$ | 3.0 | 825 | 30 | *d* | 125 |
| | 6.0 | 825 | 50 | ~200 | 140 |
| | 11.0 | 830 | 100 | ~200 | 160 |
| $[Fe(CN)_5H_2O]^{3-/2-}$ | 9.0 | 195 | 10 | 220 | 200 |
| $[Fe(CN)_5His]^{3-/2-}$ | 3.0 | 205 | 30 | 240 | 220 |
| | 31.0 | 210 | 90 | 320 | 240 |

[a] All scans at 100 mV/s. [b] $[Fe(CN)_6]^{4-/3-}$ and $[Mn(CN)_6]^{3-/2-}$ in 1 M $NaNO_3$ supporting electrolyte; $[Ru(CN)_6]^{4-/3-}$, $[Fe(CN)_5H_2O]^{3-/2-}$, $[Fe(CN)_5His]^{3-/2-}$ in 0.1 M $NaClO_4$ supporting electrolyte. [c] Peak to peak separation. [d] Indeterminate due to large background currents.

On the other hand, it seems reasonable to expect that some indication of a terminal $CN^-$ group would be obtained if it existed in reasonable concentration. The loading of surface species (~100 monolayers) is sufficiently high that minimally the outer layers should be relatively unperturbed by the nickel surface. That terminal cyanides are not observed suggests the surface is composed of a relatively ordered nickel metallocyanide lattice (crystalline) on a nickel substrate. Such a surface might be expected to have certain properties that reflect its crystalline nature. As discussed below the surfaces exhibit a unique cation specificity, which appears associated with such a structure.

**(b) Electrochemical Characterization.** Derivatized electrodes were characterized by cyclic voltammetry in aqueous electrolyte; Figure 5 shows typical results in $NaNO_3$ supporting electrolyte for $[Fe(CN)_6]^{4-/3-}$ and $[Ru(CN)_6]^{4-/3-}$. The surfaces were generated under controlled-potential conditions. As previously reported for the $[Fe(CN)_6]^{4-/3-}$ and $[Ru(CN)_6]^{4-/3-}$ couples, both of these species yield a linear dependence of peak current on scan rate as expected for a surface-bound species. For electrodes having coverages of less than $5 \times 10^{-9}$ mol/cm² (35 monolayers), extremely small peak to peak separations are observed, being close to or equal to zero for scan rates up to

(14) (a) Dows, D. A.; Haim, A.; Wilmarth, W. K. *J. Inorg. Nucl. Chem.* **1961**, *21*, 33. (b) Ghosh, S. N. *Ibid.* **1974**, *36*, 2465.
(15) Tosi, L. *Spectrochim. Acta, Part A* **1973**, *29A*, 353.

500 mV/s as predicted by theory (Table III). Higher scan rates were not investigated. Although a variety of surface derivatives have been reported to yield small peak to peak separations at scan rates of <100 mV/s, very few surfaces maintain this property at higher scan rates. In particular, it is of interest to note that Prussian Blue derivatized surfaces deviate from this pattern at scan rates >5 mV/s.[4b] This type of behavior has previously been attributed to either slow charge-transfer kinetics within the derivatizing layer or uncompensated resistance within the layer.[16] In the surfaces under consideration, independent of oxidation state, there is significant anionic character. This polyelectrolyte nature may in part overcome these effects. However, that alone is not a full explanation since Prussian Blue surfaces should be electrostatically equivalent. Explanation for the small peak to peak separation may lie in the microstructure of the interface formed. Presumably a porous interface would enhance ion diffusion rates through the layer and thus reduce ohmic losses. As is discussed below, there are indications that the nickel derivatives have a highly porous structure, while it has been suggested that Prussian Blue surfaces have fairly strict steric requirements. Charge mobility and low resistance in the nickel surfaces may be enhanced by a population of mobile $Ni^{2+}$ within the layer, generating what is effectively a solid-state electrolyte at the interface. Indirect evidence that this may be occurring is found in the observation that electrodes cannot be kept indefinitely in the ferric form under open-circuit conditions. Rather, the derivative is slowly reduced. Presumably the reducing agent is nickel metal, and thus nickel ion generation within the derivatizing layer is fairly facile.

Finally, it should be noted that the surface waves in $Na^+$- or $K^+$-containing electrolyte are very narrow having on the average a full width at half height of ~110 mV (see Table III). This approximates the theoretical value for noninteracting, one-electron surface sites of 90 mV.[17] Most surfaces reported to date have significantly larger peak widths. This has been attributed to repulsive site–site interactions.[17-20] On the other hand, Prussian Blue surfaces have been reported to have a 50-mV peak width indicating attractive interactions.[4b] Therefore, the observed peak width may be explained in terms of a fortuitous cancellation of attractive and repulsive interactions. This latter possibility appears more likely, since as previously shown in ref 7 changing the supporting electrolyte can drastically alter the peak shape, generating a surface with definite site–site interactions.

In one respect the surfaces do not exhibit ideal behavior. Low-coverage electrodes show a nonzero base line at anodic potentials, suggesting a second electrochemical process not related to the derivative electrochemistry. This may be associated with direct surface oxidation to generate a small amount of $Ni^{2+}$ or the reversible oxidation of $Ni^{II}(OH)_2$ to $Ni^{III}(O)OH$.[9] Whatever the exact process, it does not seem to cause a deterioration in the $[M(CN)_6]^{4-/3-}$ surface wave or the surface itself.

As mentioned earlier it is possible to construct interfaces containing more than one species either by potentiostating in an electrolyte containing both complexes or by consecutive anodization processes. This is demonstrated by using the second process in Figure 6. Independent of the method used to construct the interface, the same cyclic voltammetric response is observed. This is in contrast to Murray's[21] results on multiple-layer polymer interfaces that demonstrate rectifying behavior, suggesting that a laminar structure does not result. This observation is consistent with the formation of a highly porous surface structure.

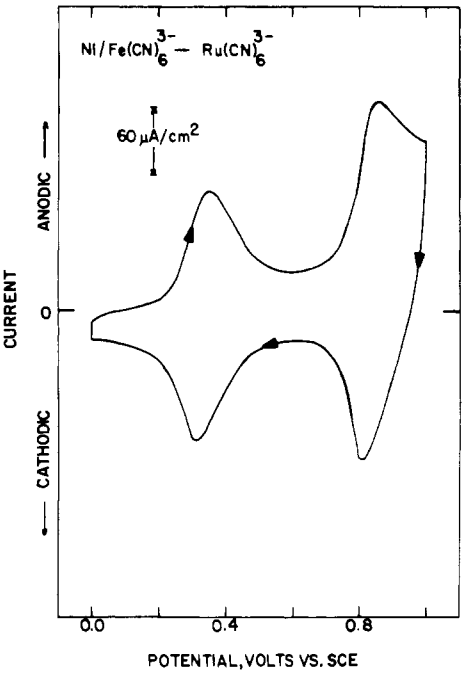


**Figure 6.** Cyclic voltammogram in 0.1 M $NaNO_3$ at 100 mV/s of a nickel electrode derivatized in a solution containing $5 \times 10^{-3}$ M $[Fe(CN)_6]^{4-}$ and $5 \times 10^{-3}$ M $[Ru(CN)_6]^{4-}$. The waves at +0.32 V vs. SCE correspond to the $[Fe(CN)_6]^{4-/3-}$ couple, and those at +0.82 V vs. SCE to the $[Ru(CN)_6]^{4-/3-}$ couple.

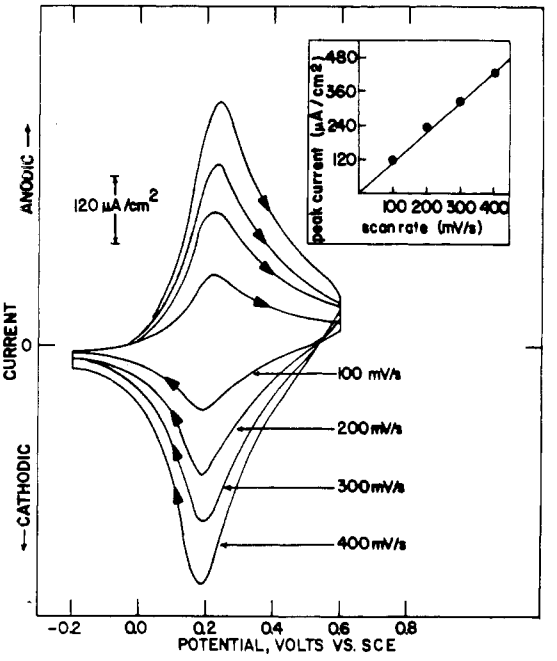


**Figure 7.** Cyclic voltammogram of nickel modified with $[Fe(CN)_5His]^{3-}$. Scans are in 0.1 M $NaNO_3$. Inset shows the linear dependence of anodic peak current on scan rate. Note the wave width in comparison to the $[Fe(CN)_6]^{4-/3-}$-derivatized electrode.

Results similar to those discussed for the various octahedral complexes are also obtained for substituted cyanoferrate

(16) Daum, P.; Murray, R. W. *J. Phys. Chem.* **1981**, *85*, 389.
(17) Laviron, E. *J. Electroanal. Chem. Interfacial Electrochem.* **1981**, *122*, 37.
(18) Daum, P.; Lenhard, J. R.; Rolison, D.; Murray, R. W. *J. Am. Chem. Soc.* **1980**, *102*, 4649.
(19) Wrighton, M. S.; Palazzotto, M. C.; Bocarsly, A. B.; Bolts, J. M.; Fischer, A. B.; Nadjo, L. *J. Am. Chem. Soc.* **1978**, *100*, 7264.
(20) Bolts, J. M.; Bocarsly, A. B.; Palazzotto, M. C.; Walton, E. G.; Lewis, N. S.; Wrighton, M. S. *J. Am. Chem. Soc.* **1979**, *101*, 1378.
(21) Abruna, H. D.; Denisevich, P.; Umana, M.; Meyer, T. J.; Murray, R. W. *J. Am. Chem. Soc.* **1981**, *103*, 1.

complexes. All of the complexes that were surface attached $(Fe(CN)_{6-x}L_x]^{n-}$; L = NO, $H_2O$, L-histidine, $NH_3$, 1,2-cyclohexyldiamine) were electrochemically active with the exception of nitroprusside, a material known to only yield reversible electrochemistry under basic conditions (where the present system is unstable). Of major interest is the interaction of $[Fe^{III}(CN)_5(His)]^{2-}$ with the nickel interface. The asymmetry of this molecule might be expected (due to the polycrystalline nature of the surface) to induce different surface interactions than the previously discussed octahedral surface species. A cyclic voltammetric analysis of this surface is found in Figure 7. This species yields an $E_{1/2}$ value ~100 mV negative of the $[Fe(CN)_6]^{3-}$ surface species, indicating (along with the IR data) that it is indeed the desired complex and not a $[Fe(CN)_6]^{4-/3-}$ impurity in the derivatizing solution. The $E_{1/2}$ value is also 15 mV positive of surface-bound $[Fe(CN)_5H_2O]^{3-/2-}$, the synthetic precursor of this species, veryifying that the appropriate molecule is surface attached. The major difference between the electrochemical response of this surface and those previously discussed is found in the large peak width. Like the other surfaces, this interface yields a linear scan rate dependence and small peak to peak separation, indicating that it is surface bound. The large peak width suggests intermolecular interactions of a repulsive nature, as might be expected for a sterically bulky molecule such as the histidine derivative. Presumably the surface material does not pack as well as the octahedral species, leading to a degree of disorder and lattice distortion not found with the octahedral surfaces.

As demonstrated by repetitive cyclic voltammetry, the surfaces show good stability; however, some deterioration in the amount of surface-attached material is noted after prolonged cycling. For example, the $Ni/Fe(CN)_6^{4-/3-}$ surface loses ~50% of its surface material after ~3000 oxidation–reduction cycles at 100 mV/s (14 h of cycling). However, this deterioration can be arrested by adding a small amount of $[Fe(CN)_6]^{3-}$ to the electrolyte. We have cycled derivatized electrodes in electrolyte containing $3 \times 10^{-5}$ M $[Fe(CN)_6]^{3-}$ for over 18 000 cycles (50 h) with only a 10% loss in surface material. Stability under dry storage is found to be quite acceptable. Electrodes stored in air at room temperature for several months yield good cyclic voltammetric surface waves, showing only a few percent loss in surface material.

That the surfaces themselves yield stable redox behavior is surprising in light of the fact that even in nonaqueous solvents one cannot obtain stable results for a nonderivatized nickel electrode.[8] This is apparently due to efficient formation of insulating surface oxides via reaction of small amounts of water with the nickel interface. The presence of surface $[M(CN)_6]^{4-/3-}$ complexes apparently precludes this process as long as an excessive positive potential is not applied to the electrode (>1.0 V vs. SCE). This is demonstrated in Figure 8, which compares the behavior of a nonderivatized and a $[Fe(CN)_6]^{4-/3-}$-derivatized electrode in the potential region from 0.0 V vs. SCE to +0.7 V vs. SCE. Initially, the nonderivatized electrode exhibits a large current in this region, presumably due to surface oxide formation. Upon further cycling, the current rapidly drops off to a negligible value indicating the passivation of the electrode. These results are consistent with those of recently reported experiments using galvanostatic methods in pH 7.6 buffered aqueous solution.[10] On the other hand, the $[Fe(CN)_6]^{4-/3-}$-derivatized nickel interface shows only current associated with the derivatized surface redox couple plus a small base line current, as previously noted.

This stabilization is demonstrated for the oxidation and reduction of solution ferrocene in Figure 9. A nondried acetonitrile/TBAP (tetrabutylammonium perchlorate) electrolyte is employed. Note the nonderivatized electrode yields

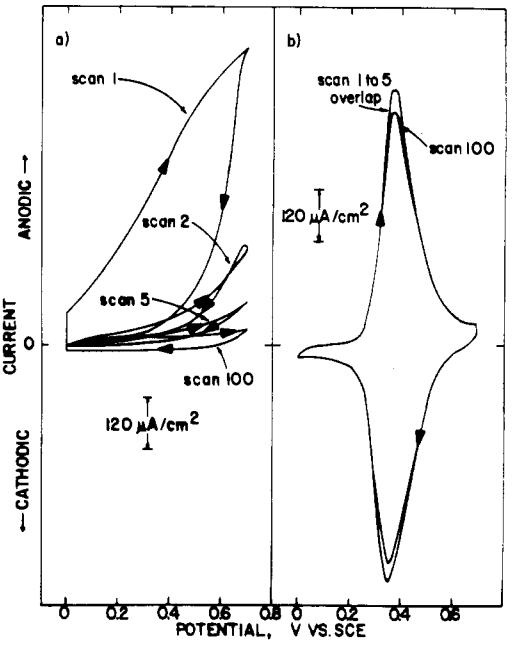


**Figure 8.** Repetitive cyclic voltammograms of nickel electrodes in 0.1 M $NaNO_3$ electrolyte (100 mV/s): (a) initial scans of a clean nickel electrode, showing passivation behavior due to oxide formation; (b) scan of a $[Fe(CN)_6]^{4-/3-}$-derivatized nickel surface, showing no passivation and a minor decrease in peak height apparently due to a slight amount of derivative decomposition.

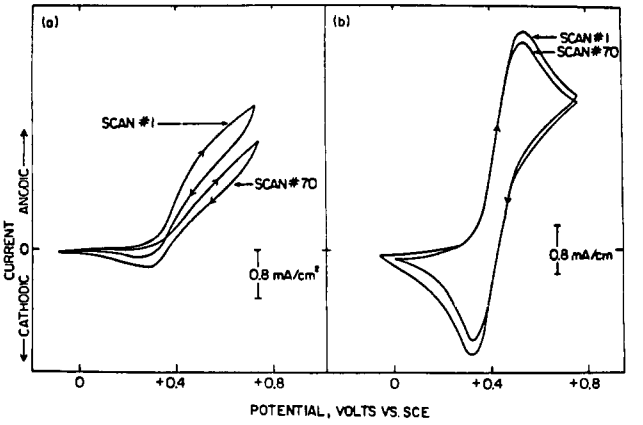


**Figure 9.** Repetitive cyclic voltammograms using (a) an untreated and (b) a $[Fe(CN)_6]^{3-}$-derivatized nickel electrode in an acetonitrile–0.1 M TBAP electrolyte containing ~10 mM ferrocene. All scan rates are 100 mV/s. The current scales have been adjusted so that the surface $[Fe(CN)_6]^{4-/3-}$ wave is not visible. The wave in part b corresponds to the reversible one-electron oxidation of solution ferrocene and is a response identical with that observed with a platinum electrode in the same solution.

an unstable cyclic voltammogram, decreasing in time. Much of the anodic current is not associated with ferrocene oxidation, a fact which is demonstrated by the small cathodic current for ferrocenium reduction. On the other hand a stable, reversible cyclic voltammogram is observed with the derivatized electrode. Current scales and solution concentrations have been chosen such that the surface wave is small compared to the solution wave; thus, only current associated with the ferrocene redox couple is observed. Therefore, the $[Fe(CN)_6]^{4-/3-}$ surface not only inhibits surface corrosion/insulation processes but selectively allows ferrocene oxidation and reduction. It is interesting to note that nickel surfaces derivatized with $[Ru(CN)_6]^{4-/3-}$ do not enhance the oxidation of solution ferrocene (at potentials around the ferrocene redox potential) although surface $[Ru(CN)_6]^{4-/3-}$ does offer the same type of protection against surface oxide passivation as is demonstrated

in Figure 8 for surface-bound $[Fe(CN)_6]^{4-/3-}$. A comparison of IR and cyclic voltammetric data for $[Fe(CN)_6]^{4-/3-}$ and $[Ru(CN)_6]^{4-/3-}$ shows that they are structurally and chemically quite similar with the exception that the latter surface has an $E_{1/2}$ value 500 mV positive of the iron surface species. Therefore, the major difference in these surfaces appears to be that while surface $[Fe(CN)_6)]^{4-/3-}$ has a redox potential very close (slightly negative) to that of solution ferrocene, surface $[Ru(CN)_6]^{4-/3-}$ has a value of $E_{1/2}$ significantly positive of the solution species. These observations suggest that the mechanism of surface protection is not based simply on a surface coating, which excludes reagents capable of forming passivating nickel oxides (physical protection), but is associated with mediated electron transfer through the surface derivative. The existence of such a charge-transfer mechanism would suggest that highly reaction-specific surfaces can be synthesized. Current investigations center on analyzing the specific mechanisms of this process. These results will be reported in the future.[22]

Evidence also exists that surface metallocyanide complexes, besides acting as surface-protection reagents, can endow the nickel electrode with a degree of electrocatalytic capability. For example, the $Ni/Fe(CN)_6^{4-/3-}$ surface is observed to show an onset for the oxidation of ascorbic acid at potential near the onset of $Fe(CN)_6^{4-}$ surface oxidation in $NaNO_3$ supporting electrolyte (+0.2 V vs. SCE). On the basis of the position of peak potentials, this is 350 mV negative of the potential where ascorbic acid is oxidized at a native nickel surface.[35] As in the case of ferrocene, the potential at which ascorbic acid oxidation is observed is dependent on the redox potential of the surface-attached species. Thus, in the case of a $Ni/Ru(CN)_6^{4-/3-}$-coated surface no electrocatalysis is observed since ascorbic acid oxidation on native nickel occurs positive of the surface $E_{1/2}$. On the other hand, $Ni/Fe(CN)_5H_2O^{3-/2-}$-coated surfaces ($E_{1/2}$ = +0.20 V vs. SCE) show an ascorbic acid wave negative (~100 mV) of that observed on $Ni/Fe(CN)_6^{4-/3-}$ ($E_{1/2}$ = +0.36 V vs. SCE) surfaces.

**(c) Electrolyte Effects.** As we have recently noted, perhaps one of the most stimulating aspects of these interfaces is their interaction with the electrolyte.[7] It has been known for quite some time that both the thermodynamics and kinetics of $[Fe(CN)_6]^{4-/3-}$ in solution are a fairly strong function of electrolyte and supporting electrolyte. For example, changing the solvent employed can shift $E_R$ more than 1 V.[23] Various mixtures of acetonitrile and water can be used to continuously vary $E_R$ over a 1.3-V range. This effect has been associated with solvent (acceptor) interaction with the nitrogen lone pair.[24] An identical effect has recently been observed for $[Fe(CN)_6]^{4-/3-}$, electrostatically bound to an electrode surface via a charge-transfer polymer.[27] Similarly, various cations are found to shift the solution $[Fe(CN)_6]^{4-/3-}$ $E_R$.[25] This shift is based both on the specific cation and on the concentration of the cation and has been associated with ion-pair formation with $[Fe(CN)_6]^{4-}$ shifting the Nernstian equilibrium: the effect is limited to ~50 mV. More dramatically, it has been observed that the nature of the cation present can change the self-exchange rate for the $[Fe(CN)_6]^{4-/3-}$ couple as well as the heterogeneous charge-transfer rate at an electrode.[26] It has been suggested that this is due to the formation of an outer-sphere complex, containing a bridging cation, during the charge-transfer process. All of these effects have been associated with the nitrogen lone pair. The IR data presented earlier suggest that such an agent would not be operative in the present system since the nitrogen lone pair is bonding with respect to Ni(II). As previously reported, this expectance is borne out by the lack of a strong solvent dependence for the derivatized surface.[7] The value of $E_{1/2}$ varies less than 50 mV between acetonitrile/0.1 M $LiClO_4$ and water/0.1 M $LiClO_4$ electrolytes. The same is true in alcohol- and dichloromethane-containing electrolytes.

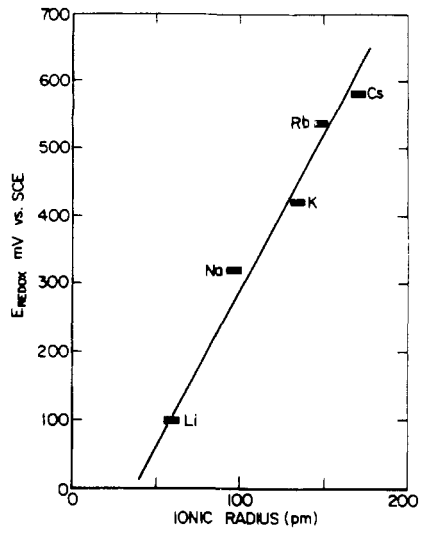


**Figure 10.** Plot of $E_R$ for surface-bound $[Fe(CN)_6]^{4-/3-}$ as a function of the effective ionic radius of the supporting electrolyte cation. All cations are held at 0.1 M bulk concentration. Values of $E_R$ are obtained from the cyclic voltammetric peak value, assuming $E_R = E_{1/2}$.

Most interestingly, however, is the observation that the surface redox potential is a strong function of the supporting electrolyte cation. This is illustrated in Figure 10 for the alkali-metal cations, which shift $E_R$ linearly with cation radius. The effect is *more the 1 order of magnitude larger than that observed with the anion complex in solution (50 mV)*. The change in $E_R$ from $Li^+$ to $Cs^+$, 600 mV, rules out a simple shift in the Nernstian equilibrium as the source of this phenomenon. Further, the lack of an accessible nitrogen lone pair indicates a totally different mechanism is operating here. The phenomenon responsible for the observed behavior should not be confused with previously presented results, which indicate a shift in the surface $E_R$ with the concentration of supporting electrolyte (not the cation present) observed with Prussian Blue surfaces[4,5,30] or the shift in $E_R$ reported for Nafion/tetrathiofulvene films with variations in solution anions (~50–100 mV).[31] Both of these effects can easily be explained by assuming simple Nernstian behavior and the presence of contact ion pairing. Two explanations would appear possible. The first is to consider the interface as a solid-state membrane in which the actual potential would be a function of the electrode potential, a diffusion potential, and a junction potential between the surface and the electrolyte. Different cations would affect these latter potentials making the surface $E_R$ appear to shift. In fact the potential shift would be due

(22) A discussion of the mechanism of electrocatalysis at nickel surfaces derivatized with various silanes exhibiting similar chemistry recently appeared.[8]
(23) Gritzner, G.; Danksagmuller, K.; Gutmann, V. *J. Electroanal. Chem. Interfacial Electrochem.* **1976**, *72*, 177.
(24) Gutmann, V.; Gritzner, G.; Danksagmuller, K. *Inorg. Chim. Acta* **1976**, *17*, 81.
(25) (a) Eaton, W. A.; George, P.; Hanania, G. I. H. *J. Phys. Chem.* **1967**, *71*, 2016. (b) Hanania, G. I. H.; Irvine, D. H.; Eaton, W. A.; George, P. *Ibid.* **1967**, *71*, 2022.
(26) Peter, L. M.; Durr, W.; Bindra, P.; Gerischer, H. *J. Electroanal. Chem. Interfacial Electrochem.* **1976**, *31*, 71.
(27) Braun, H.; Storck, W.; Doblhofer, K. *J. Electrochem. Soc.* **1983**, *130*, 807.
(28) Kourim, V.; Rais, J.; Million, B. *J. Inorg. Nucl. Chem.* **1964**, *26*, 1111.
(29) Saraswat, I. P.; Srivastava, S. K.; Sharma, A. K. *J. Colloid Interface Sci.* **1981**, *84*, 163.
(30) Spierko, L. M.; Kuwana, T. *J. Electrochem. Soc.* **1983**, *130*, 396.
(31) Henning, T. P.; Bard, A. J. *J. Electrochem. Soc.* **1983**, *130*, 613.

to the uncompensated resistance associated with the interface potentials. The second possible explanation is that different cations interact with the surface species in a previously unobserved manner so as to perturb the electronic energy of the surface species and thus $E_R$. The interaction would have to be reversible since the change in surface $E_R$ is reversible and reproducible with electrolyte. The first explanation appears highly unlikely since it is possible to generate a voltammogram having two-surface waves by using a mixed electrolyte as is demonstrated in the cyclic voltammetry in ref 7. A potential gradient at the interface should affect all species equally; thus, only one peak should be observable. Therefore, at this time the second explanation is preferred. Currently, we are investigating the exact mechanism by which such an effect can be induced.

Besides a direct effect on $E_R$, there exist other surface-supporting electrolyte interactions of importance. We have previously noted that the rate of charge transfer can be altered by changes in the cation.[7] Similar results have been reported for Prussian Blue derivatized electrodes, with the exception that cation response is quite limited.[4b,5c,30] This behavior has been associated with a steric effect that excludes hydrated ions larger than $K^+$ from entering the Prussian Blue derivative and has lead to the idea that these surfaces are polycrystalline in nature having specific cavity or pore sizes.[5c,30] The derivatized nickel surfaces exihibit a similar size selectivity; however, it is not as exaggerated as has been noted for the Prussian Blue surfaces. All of the alkali cations yield fairly reversible cyclic voltammograms. However, $Li^+$, the largest hydrated alkali cation, yields rather broad waves in comparison to the other alkali cations. Similarly if an extremely large cation containing salt such as tetrabutylammonium is used as the supporting electrolyte, only a very small and distorted cyclic voltammetric response is observed, indicating that the cation cannot penetrate the derivative and supporting the conclusions that the nickel surfaces are sterically and thus structurally rigid.

We also find that there exists a definite surface affinity for different cations. This has been established from competition experiments in which an aliquot of solution containing one cation is added to an electrochemical cell containing a 0.1 M concentration of another cation. The process is continued until cyclic voltammetry indicates nearly total surface dominance by the added cation. The final concentration of cations in the electrolyte is used to rank the cations with respect to surface affinity. For example, addition of $CsNO_3$ solution to a 0.1 M $NaNO_3$ electrolyte causes the cyclic voltammogram to shift totally to the "$Cs^+$" surface wave at concentrations of $Cs^+$ above 0.05 M. However, one must add massive excesses of $NaNO_3$ to cause a "$Cs^+$" surface wave established by placing the electrode in 0.1 M $CsNO_3$ to be shifted to the "$Na^+$" surface wave potential. This clearly indicates a preference for $Cs^+$ over $Na^+$. $[Fe(CN)_6]^{4-/3-}$- and $[Ru(CN)_6]^{4-/3-}$-derivatized electrodes indicate the following surface affinity ranking: $Cs^+ > Rb^+ > K^+ \sim NH_4^+ > Na^+ > Ba^{2+} > Li^+ > TBA^+$. As can be seen from Figure 10, this ordering parallels the observed change in $E_R$. The cation selectivity is not at all surprising in light of the fact the Prussian Blue and its analogues are well-known inorganic ion exchangers.[29] Such materials show the same affinity ranking as shown above. This has been related to the size of the hydrated cation and thus its ability to enter the crystal lattice.[30] It therefore appears that the derivatizing layer presents in general the same sort of structure as found in the bulk material. There does exist some degree of synthetic control over the exact structure generated via the potential selected for surface formation. Cyclic voltammetry indicates that the derivatizing layer charge-transfer rate in $LiClO_4$ electrolyte is a function of the potential at which the interface is initially formed. Surfaces formed at potentials positive of 2.0 V vs. SCE show more sluggish electron-transfer rates than those formed at more negative potentials. In $CsNO_3$ electrolyte no formation potential dependence is observed, however. That the smaller hydrated $Cs^+$ penetrates the surface independent of the synthetic procedure while the larger hydrated $Li^+$ shows a distinct dependence on surface-formation methodology implies that surface microstructure can be controlled over a limited range.

The differential cation affinity properties of the surface-attached material can be utilized to generate an interfacial system capable of overcoming the activation barrier to ion exchange. If an $[Fe(CN)_6]^{4-/3-}$-derivatized electrode that has previously been immersed in a $Cs^+$-containing electrolyte and removed from that electrolyte in the $[Fe(CN)_6]^{4-}$ form is washed and placed in a $Na^+$-containing electrolyte, only very slow ion exchange is observed. Cyclic voltammetry indicates a half-life for the $Cs^+$-containing surface of $\sim$1 h. However, if the electrode is potentiostated such that the $[Fe(CN)_6]^{3-}$ oxidation state is formed followed by the regeneration of $[Fe(CN)_6]^{4-}$ in the $Na^+$-containing electrolyte, rapid exchange of the $Cs^+$ is observed. Oxidation of the surface complex requires a decrease in the surface $Cs^+$ concentration. Once this has occurred the large $[Na^+]$ to $[Cs^+]$ ratio in solution favors displacement by $Na^+$ upon reduction. The net effect is to couple the electrode potential to the exchange activation energy. Thus, the interface represents an ion switch in which the ion affinity of the derivatizing layer can be modulated.

## Summary

Nickel electrodes can be derivatized with a variety of complexes of the form $[M(CN)_{6-x}L_x]^{n-}$. Empirically, any complex that forms a precipitate when mixed with $Ni^{2+}$ in solution can be employed to derivatize the nickel interface. The derivative so formed consists of a polycrystalline lattice composed of $Ni^{II}$ and $M^{II/III}$ centers bonded through bridging cyanide ligands. On the basis of stoichiometric considerations, a net anionic charge is assigned to the surface lattice. This charge is compensated for by either nickel ions from the surface or cations in solution. That solution cations are to some extent responsible for the charge compensation is concluded on the basis of cyclic voltammetric changes associated with changing the supporting electrolyte. Therefore, the overall interfacial charge transfer for an octahedral surface-bound metal–cyanide complex can be described by eq 1, where R represents cations

$$R_x[Ni^{II}(NC)M^{III}(CN)_5]_y + e^- \rightarrow R_z[Ni^{II}(NC)M^{II}(CN)_5]_y \quad (1)$$

available from solution or $Ni^{2+}$ ions. Previously reported X-ray analysis of bulk $[Ni^{II}Fe^{II}(CN)_6]^{2-}$ indicates that the lattice can accommodate either $Ni^{2+}$ or alkali ions as the cationic charge centers.[32]

Surfaces can be synthesized in a precise and reproducible manner by controlling electrode potential, derivatization time, and reagent concentration. Surface stability is quite reasonable and exceeds that of many other chemically modified surfaces if a small amount of the anion complex is added to the electrolyte. The derivatized surfaces exhibit an ability to suppress surface corrosion as well as to enhance certain interfacial charge-transfer reactions. Further, they demonstrate a degree of cation selectivity with respect to both charge-transfer kinetics and surface thermodynamics not previously reported. This leads to the conclusion that the derivatized interface expresses both chemical and physical effects on the interfacial charge-transfer process and that surface microstructure can be as influential as the chemical nature of the surface species. Finally, we note that such surfaces are of possible interest with

(32) Rigamonti, R. *Gazz. Chim. Ital.* **1938**, *68*, 803.

respect to the construction of both ion-sensing interfaces and electrosynthetic cells.

## Experimental Section

**Materials.** Nickel electrodes consisted of Ni wire of 0.63-mm diameter (Alfa). Nickel plate electrodes used for IR studies were 0.125-mm thick (Alfa) having an area of 1 $cm^2$. Inco 255 Ni powder was used for UV-vis studies. Reagent grade chemicals were used as derivatizing agents and supporting electrolytes. $Na_3Fe(CN)_5H_2O$ was made by dissolving $Na_3Fe(CN)_5NH_3$ in distilled water at pH 4.[33] $[Fe(CN)_5His]^{2-}$ solution was made by stirring a mixture of 50 mL of 0.2 M $Na_3Fe(CN)_5H_2O$, 50 mL of 6% $H_2O_2$, and 2.3 g of L-histidine in the dark for 45 min at about 5 °C. A catalytic amount of $MnO_2$ was added at the end of the reaction to decompose excess $H_2O_2$.[34]

**Electrochemistry.** A single-compartment cell with a large Pt-mesh counterelectrode and SCE as reference was used. Measurements were made with a PAR Model 174A potentiostat and a PAR Model 175 programmer. Electrodes were abraded with 150 metalite cloth and washed with distilled water before derivatization. After derivatization, they were wiped with a Kimwipe and washed with distilled water to remove loosely adhering substances. Data were recorded on a Houston Instruments 2000 recorder.

Ideal electrodes were made by potentiostating the Ni-wire electrodes at 1.0 V vs. SCE for 50 s in an electrolyte containing 0.1 M $NaNO_3$ and 0.005 M $[Fe(CN)_6]^{3-}$. By appropriate increase of potentiostating voltage, time, and concentration of $[Fe(CN)_6]^{3-}$, larger coverage electrodes were obtained as desired.

**Spectroscopy.** Diffuse-reflectance FT IR spectroscopy was carried out on a Digilab FTS.20C spectrometer with a diffuse-reflectance attachment. A derivatized Ni-plate electrode was used as the sample while a nonderivatized abraded Ni plate served as the reference. The model compounds were used as powders and referenced against KBr. UV-vis spectra were recorded on a Hewlett-Packard 8540A UV-vis spectrometer.

**Acknowledgement** is made to the Dreyfus Foundation for partial support of this work through a newly appointed Young Faculty Grant. Professor Kalman Burger is thanked for informative discussions that helped fuel this work at its early stages.

**Registry No.** $K_3Fe(CN)_6$, 13746-66-2; $Fe(CN)_6^{3-}$, 13408-62-3; $Na_3Fe(CN)_5H_2O$, 14100-31-3; $[Fe(CN)_5His]^{2-}$, 88181-56-0; $Ru(CN)_6^{4-}$, 21029-33-4; $KNiFe(CN)_6$, 53295-14-0; $K_4Fe(CN)_6$, 13943-58-3; $K_2NiFe(CN)_6$, 13601-16-6; $Na_2Fe(CN)_5H_2O$, 14220-67-8; $NiFe(CN)_5H_2O$, 88181-57-1; $Na_2Fe(CN)_5NO$, 14402-89-2; $NiFe(CN)_5NO$, 14709-61-6; $NiFe(CN)_5His$, 88181-58-2; $K_4Ru(CN)_6$, 15002-31-0; $[Fe(CN)_6]^{4-}$, 13408-63-4; $[Fe(CN)_5H_2O]^{3-}$, 18497-51-3; $[Fe(CN)_5NO]^{2-}$, 15078-28-1; $[Fe(CN)_5His]^{3-}$, 60105-82-0; $Ru(CN)_6^{3-}$, 54692-27-2; $[Fe(CN)_5H_2O]^{2-}$, 19413-97-9; $Mn(CN)_6^{3-}$, 14931-63-6; $Mn(CN)_6^{2-}$, 66735-85-1; Ni, 7440-02-0; Cs, 7440-46-2; Rb, 7440-17-7; K, 7440-09-7; $NH_4^+$, 14798-03-9; Na, 7440-23-5; Ba, 7440-39-3; Li, 7439-93-2; $NaNO_3$, 7631-99-4; $TBA^+$, 10549-76-5; ferrocene, 102-54-5.

(33) Lux, H. "Handbook of Preparative Inorganic Chemistry"; Academic Press: New York, 1965; Vol. II, p 1511.
(34) Shepherd, R. E. *J. Am. Chem. Soc.* **1976**, *98*, 3329.
(35) Although unstable, in our hands the native nickel surface appears to give an oxidation peak at ~+0.65 V vs. SCE for the oxidation of ascorbic acid. This is the same potential at which we observe a peak in the ascorbic acid oxidation wave using a platinum electrode.

Contribution from the Departments of Chemistry, Massachusetts Institute of Technology, Cambridge, Massachusetts 02139, and Colorado State University, Fort Collins, Colorado 80521

# Characterization and Photochemistry of Surface-Confined Mononuclear and Trinuclear Phosphine/Carbonyl Complexes of Ruthenium(0)

DAVID K. LIU,[1] MARK S. WRIGHTON,*[1] DALE R. McKAY,[2] and GARY E. MACIEL[2]

*Received June 29, 1983*

The characterization and photochemistry of $[SiO_2]$-$LRu(CO)_4$ and $[SiO_2]$-$L_3Ru_3(CO)_9$ are reported, where $[SiO_2]$- represents high surface area (~400 $m^2/g$) $SiO_2$. Synthesis of $[SiO_2]$-$LRu(CO)_4$ and $[SiO_2]$-$L_3Ru_3(CO)_9$ is effected by reaction of $Ru(CO)_4(PPh_2CH_2CH_2Si(OEt)_3)$ or $Ru_3(CO)_9(PPh_2CH_2CH_2Si(OEt)_3)_3$ with a hydrocarbon suspension of $[SiO_2]$-. Solid-state $^{13}C$, $^{29}Si$, and $^{31}P$ CP/MAS NMR, FTIR, UV-vis photoacoustic spectroscopy, and elemental analyses establish the nature of the functionalized $[SiO_2]$-. Typical coverage of $-LRu(CO)_4$ or $-L_3Ru_3(CO)_9$ is ~$10^{-10}$-$10^{-11}$ mol/$cm^2$. Photoexcitation (near-UV) of $[SiO_2]$-$LRu(CO)_4$ suspended in hydrocarbon media results in a chemical reaction consistent with the dissociative loss of CO to give a 16-valence-electron, surface-confined species that reacts with 2-electron P-donors. The light-induced extrusion of CO can be effected and detected spectroscopically by chemical trapping in rigid media at low temperature (~90 K). Near-UV irradiation of $[SiO_2]$-$LRu(CO)_4$ at 298 K exposed to a gas gives chemistry consistent with dissociative loss of CO, also. Complete (>90%) exchange of CO for $^{13}CO$ can be effected by irradiation under 1 atm of $^{13}CO$, as monitored by FTIR/photoacoustic spectroscopy. The photochemistry of $[SiO_2]$-$L_3Ru_3(CO)_9$ involves metal-metal bond rupture; under 1 atm of CO in a solid/gas reaction or as a suspension in hydrocarbon solvent saturated with CO, $[SiO_2]$-$L_3Ru_3(CO)_9$ yields $[SiO_2]$-$(LRu(CO)_4)_3$. The surface-confined mononuclear species formed photochemically from the surface-confined trinuclear species are spectroscopically indistinguishable from the deliberately synthesized $[SiO_2]$-$LRu(CO)_4$. However, irradiation of $[SiO_2]$-$(LRu(CO)_4)_3$ leads to reassembly of the surface cluster, $[SiO_2]$-$L_3Ru_3(CO)_9$, whereas irradiation of $[SiO_2]$-$LRu(CO)_4$ yields no surface cluster. For small P-donors, L', irradiation of $[SiO_2]$-$L_3Ru_3(CO)_9$ yields $[SiO_2]$-$(LRu(CO)_3L')_3$, whereas $[SiO_2]$-$LRu(CO)_4$ yields $[SiO_2]$-$LRu(CO)_3L'$ for large and small L'. Both $[SiO_2]$-$LRu(CO)_4$ and $[SiO_2]$-$L_3Ru_3(CO)_9$ yield gas-phase CO and $CO_2$ as products when irradiated while exposed to an $O_2$-containing atmosphere.

Photochemistry at interfaces is of practical importance in several respects including solar energy conversion and imaging. Potentially, photochemistry at interfaces could have practical value in catalytic synthesis, depending on the nature of the photoreactions that can be effected. Fundamentally, study of light-induced chemistry at interfaces can lead to elucidation of reaction mechanisms and to new photoreactions. One of the exciting prospects associated with photochemistry of surface-confined molecules is that "active sites" on a surface can be prepared rationally and characterized with an arsenal of molecular-specific probes. Additionally, chemistry not possible in homogeneous solution may be possible for molecular entities attached to a surface.

In this paper, we elaborate results previously communicated[3] concerning surface-confined mononuclear and trinuclear ru-

(1) Massachusetts Institute of Technology.
(2) Colorado State University.
(3) Liu, D. K.; Wrighton, M. S. *J. Am. Chem. Soc.* **1982**, *104*, 898.

0020-1669/84/1323-0212$01.50/0 